MODELING OF OIL SPREAD ON ICE WITH SURFACE HEATING

Sharanya Nair*,¹, Tatsunori Hayashi², Hamed F. Farahani¹, Hirotaka Sakaue², Ali S. Rangwala¹

Fire Protection Engineering Department, Worcester Polytechnic Institute, MA 01609
 Department of Aerospace and Mechanical Engineering, University of Notre Dame, IN 46556
 *snair2@wpi.edu

Abstract

Oil spill in oceans is identified as a key environmental issue resulting in water contamination and major harm to marine life. These spills in ice-infested waters can be even more catastrophic as the process of ice melting is non-trivial and adds an additional complexity in determining the extent of the oil spread from the initial spill zone. The prediction of the impact and extent of the spill assists in employing the required clean-up countermeasures. A validated numerical model that simulates the oil spread is reported in this study, where the spread of an oil layer in ice is analyzed. Experiments in literature have shown that for solar radiation flux higher than 0.5 kW/m², the oil temperatures can be around 5 - 6 °C even if the ambient is at sub-zero temperature. This surface heating is simulated in the numerical model to study the effect of indepth heating of oil on the ice melting to further analyze the spreading of oil in the melt zone.

1 Introduction

Oil drilling and its subsequent transport across oceans has been the major form of fuel procurement to meet the energy needs. These technologies have a potential to cause harm to the environment in terms of oil well breakouts and spills and an effective countermeasure is sought after to minimize pollution and its effect on marine life. These spill accidents in the Arctic have even higher consequences due to the impact of the oil on ice-infested waters.

Oil spill in ice environments have been studied with respect to different aspects. Detailed studies on spreading of oil on/under ice and it fate relative to an accidental fuel source have been done in literature (summarized by Fingas and Hollebone 2003). The presence of this spreading fuel not only contaminates the ice but also accelerate the melting process of ice as the spilled oil absorbs solar radiation (Zhang et al. 2014). Additionally, in-situ burning in ice cavities (an effective countermeasure) lead to heat fluxes of more than 10 kW/m² on the fuel surface and portray enhanced melting of ice during the fuel burning (Farahani et al. 2017). Prediction models for oil spreading in ice-infested waters have been reported (Fay and Hault 1971, Glaeser et al. 1972) and in more recent studies (Yapa and Dasanayaka 2006). However, the direct application of these models involving the transient in-depth heating of fuel layers and its effect on the enhanced ice melting is non-trivial.

An experimental study to analyze the effect of an external heat flux heating the fuel layers and subsequently melting the ice has been done (Farahani et al. 2022), where the melting front and flow fields were analysed using experimental diagnostics. Based on this, the present study aims on building a numerical model where this in-depth heating of fuel layers and its effect on melting of adjacent ice can be studied systematically. In literature, numerical fate models have been developed for oil spills in ice waters (Li et al. 2013) in the absence of any transient fuel heating. The present numerical model will act as a preliminary study which will be accompanied by development of prediction models for oil spreading in ice under the effect of the excess heating.

2 Numerical Methodology

Figure 1 shows the computational domain for modeling the ice melting adjacent to heated fuel layers as built on Ansys Fluent. Experiments performed by Farahani et al. (Farahani et al. 2022) have been considered for model verification and validation. In the experiment, a 20 mm thick ice slab is placed in a 70 mm \times 70 mm square borosilicate container filled with n-dodecane fuel (Farahani et al. 2022) occupying 50 cm of the container initially. An IR radiation panel heats the fuel from the top at heat fluxes (HF) amounting to 1, 3.1 and 11 kW/m².

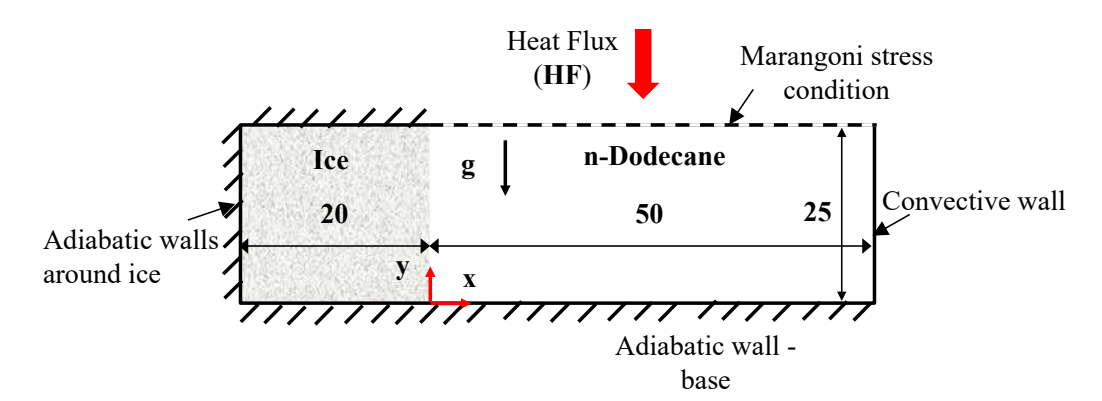


Figure 1: Computational domain for ice melting model (Recreating the experimental setup of Farahani et al. (Farahani et al. 2022))

2.1 Model Overview

For numerical modeling, a two-dimensional domain is considered as shown in Figure 1. The origin of the computational domain is placed at 20 mm from the left wall, which is also the initial thickness of the ice. A Volume of Fluid (VOF) model is prescribed in a pressure-based solver in Ansys Fluent to simulate this multiphase problem. An explicit scheme is used with n-dodecane being the primary phase and ice being the secondary phase. The solidification/melting model is incorporated by specifying the latent heat of melting (334 kJ/kg) and the melting point of ice (0 °C). Variable thermophysical properties of density, specific heat, thermal conductivity, and viscosity are incorporated for all the phases (n-dodecane, ice, melt water) using piecewise-linear fits as obtained from NIST WebBook data (Linstrom and Mallard).

2.2 **Boundary Conditions**

The boundary conditions in the model replicate the experimental conditions. The ice walls are adiabatic, while convective boundary is specified at the fuel side wall as shown in Figure 1. The base of the glass container is assigned an adiabatic condition as well. Marangoni stress condition is prescribed at the fuel surface by specifying surface tension gradient as -7.8 \times 10⁻⁵ N/m-K for n-dodecane.

The implementation of fuel heating condition from the radiation panel is non-trivial considering the fuel transmittance and an in-depth absorption coefficient. Based on in-depth heating of the fuel, the heat flux at a location y' from the fuel surface can be expressed as

$$\dot{Q}'(y) = \chi \times HF \times \exp(-\mu y') = \chi \times HF \times \exp[-\mu(L-y)]$$
where $y' = L - y$ χ represents the transmissibility of the fuel and μ (1)

equation (1), it should be noted that χ and μ are unknown. To model this accurately, the experimental temperature data is used to simulate the heating conditions. The temperature profile is available at x = 15 mm (Farahani et al. 2022). A simple one-dimensional model is used to solve the energy equation to evaluate the temperature variation in n-dodecane fuel layer in the absence of ice. The in-depth heating is modeled using a heat generation term $\dot{Q}^{\dagger}(y)$, which is a function of y as shown in equation (2). MATLAB is used to solve this equation numerically using explicit finite difference method. The energy equation is given by,

$$\frac{\partial T}{\partial t} = \alpha \frac{\partial^2 T}{\partial y^2} + \frac{\dot{Q}^{"}(y)}{k} \tag{2}$$

where, α is the thermal diffusivity of n-dodecane. The volumetric source term is given by,

$$\dot{Q}'''(y) = \dot{Q}''(y) \times \frac{Area}{Volume} = \dot{Q}''(y) \times \frac{\Delta \times 1}{\Delta \times \Delta \times 1} = \frac{\dot{Q}''(y)}{\Delta}$$
(3)

where Δ is the grid spacing in MATLAB model and $\dot{Q}''(y)$ is a function of y', HF, χ , and μ .

Since HF is known, χ and μ are iterated systematically until the temperature profiles coincide with the experimental data as shown in Figure 2(a). The lines in Fig. 2(a) represent the predicted temperature profile in n-dodecane fuel using the 1D MATLAB model. The value of χ is found to be 0.0235 and μ is 450 in order to match the temperature profiles for all three heat flux cases. Thus, using equations (1) and (3), the volumetric heat input in W/m³ would be given by

$$\dot{Q}'''(y) = \frac{\dot{Q}'}{\Delta} = \frac{0.0235 \times HF \times \exp(-450y')}{0.00025} = 94 \times HF \times \exp[-450(L-y)]$$
 (4)

This heat source value is plotted as shown in Fig. 2(b) for the different heat flux cases of 1, 3.1 and 11 kW/m² modeling the in-depth heating by the radiation panel. It is to be noted that the volumetric heat value is grid-independent, and the values as shown in Fig. 2(b) can be implemented depending on the heat flux (HF) value. The value of $\Delta = 0.25$ mm has been used only in the MATLAB model to obtain the values of γ and μ .

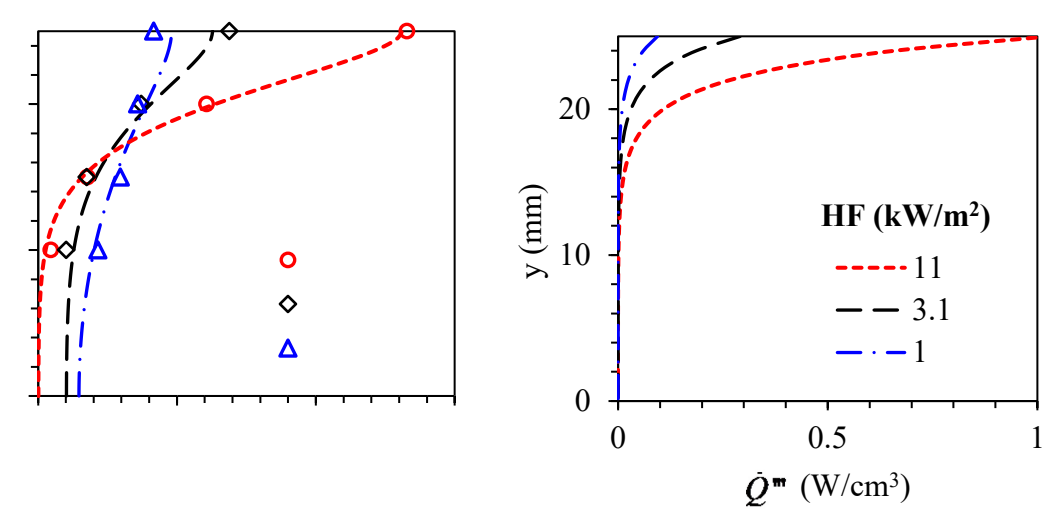


Figure 2: (a) Comparison of in-depth temperature profile for L = 0.025 m, χ = 0.0235, μ = 450, Δ = 0.25 mm (symbols - experiment, lines - 1D model), and (b) in-depth volumetric heat source for different heat flux cases,

The modified energy equation is shown in equation (5) where the volumetric source term is implemented. In Ansys Fluent, this source term is accounted for by incorporating a user defined function where, \dot{Q}^{III} is obtained from equation (4) or Fig. 2(b).

$$\frac{\partial (\rho H)}{\partial t} + \nabla \cdot (\rho \vec{V} H) = \nabla \cdot (k \nabla T + \vec{\tau} \vec{V}) + \dot{Q}^{"}$$
(5)

The continuity equation accounting for phase change and momentum equations are solved along with the energy equation. Transient cases are run by initializing ice to be 20 mm thick with 50 mm of n-dodecane fuel adjacent to it. The ice temperature is initially set at -1 2 °C and fuel temperature is set to 0 °C replicating the experimental conditions. The volumetric source is input as a use defined function to model the in-depth fuel heating. An adaptive time step procedure is implemented such that the global Courant number is less than 0.25. The initial time step is 0.001 s and this time step is varied depending on the Courant number evaluated every time step. This adaptive method is implemented to reduce the computational time and still obtain converged results through multiple iterations per time step. The normalized residuals for continuity, momentum equations are set to converge when the value is less than 10⁻³. The criteria for convergence for the energy equation is the normalized residual being less than 10⁻⁶.

3 Model Validation

Figure 3 shows the predicted profiles of ice melting front at time instant of t=2 minutes from the initial condition for heat flux values of 3.1 and 11 kW/m². It is to be noted that x=0 mm is the initial location of the ice. The experimental data obtained (Farahani et al. 2022) is used for the validation of the model. The melting profiles are seen to compare well with the experimental data. It is observed that the lateral ice melting is more significant near the fuel surface at y=25 mm, especially for 11 kW/m² case. It is noted that there is a discrepancy in the predicted melting front beyond x=0 mm. This discrepancy is attributed to the fact that the rising fuel surface due to accumulation of melting water is not accounted for in the model. However, the predicted melting front profile and its variation with heat flux gives confidence in the numerical model for further analysis.

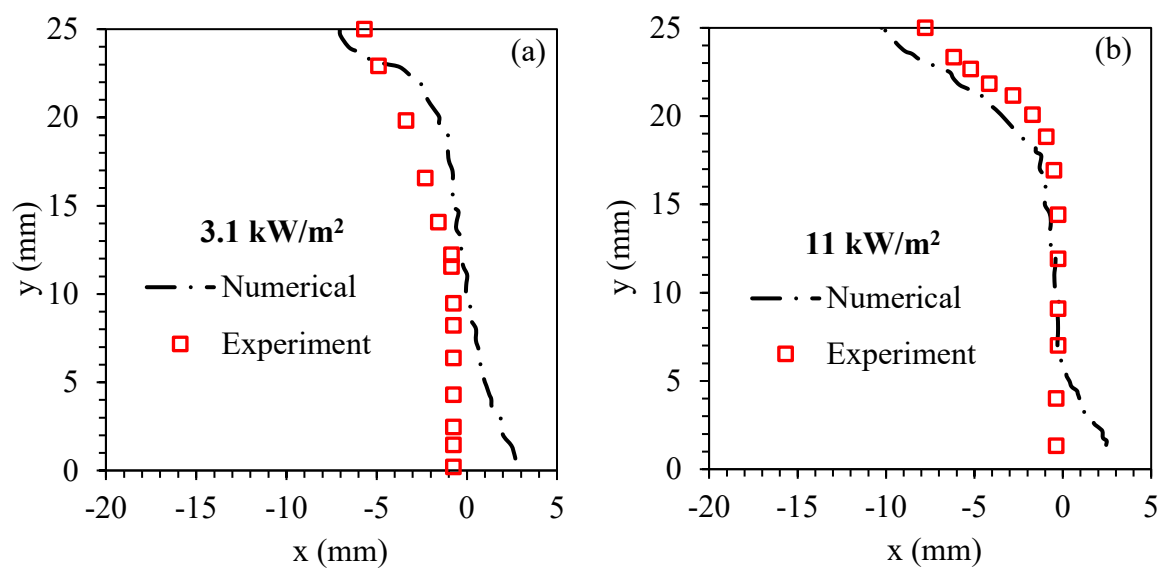


Figure 3: Ice melting profile after time instant of t = 2 minutes for a heat flux of (a) 3.1 kW/m² and (b) 11 kW/m²; experimental data from Farahani et al. 2022

Moreover, the melting intrusion velocity which is the rate at which the melting front travels in ice is evaluated and tabulated as shown in Table 1 for the two different heat flux conditions. The predicted values are in close comparison to the experimental values showing that the model is well validated for predicting the ice melting front.

Table 1: Melting intrusion velocity for a heat flux of (a) 3.5 kW/m² and 11 kW/m²

	3.1 kW/m ²	11 kW/m ²
Experiment	2.8 mm/min	4.7 mm/min
Numerical	3.5 mm/min	4.9 mm/min

Additionally, grid independence study is done to analyze the effect of the grid size on the melting prediction. Figure 4(a) shows the variation in melting front profile for the three different uniform grids and Fig. 4(b) shows the fuel temperature profile for the different grids. It is seen as the mesh is refined the profiles tend to coincide and intermediate and fine meshes show similar variation in both melting front and temperature profiles. Thus, for this study, the intermediate mesh has been used to optimize the computational time and cost.

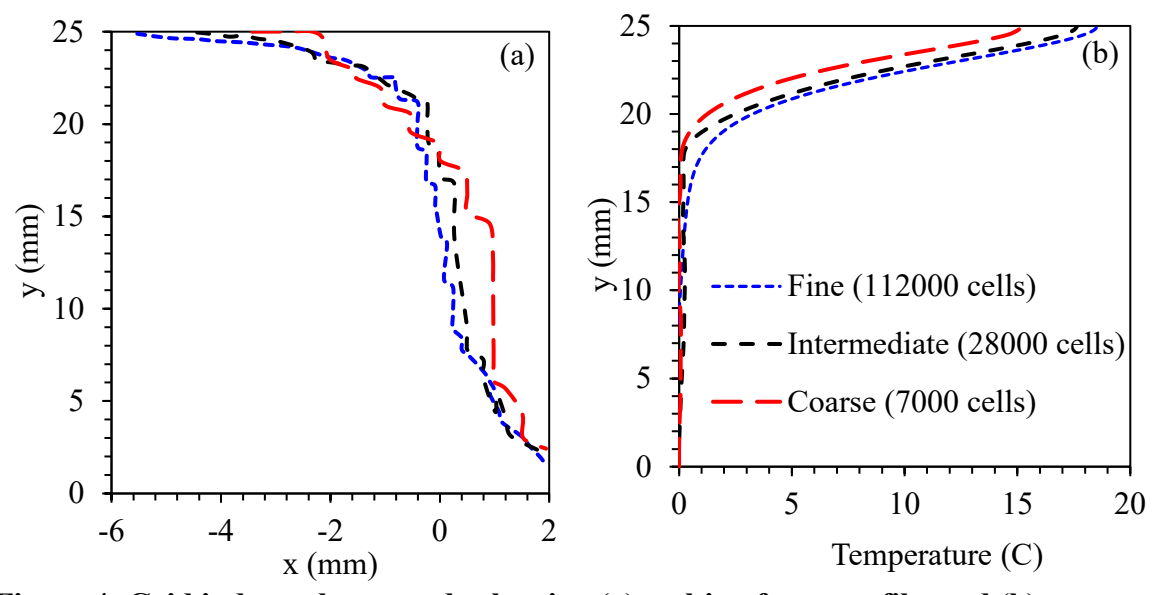


Figure 4: Grid independence study showing (a) melting front profile, and (b) temperature profile at x = 15 mm; time instant t = 1 minute, heat flux = 11 kW/m²

4 Results and Discussion

The process of fuel heating and ice melting is analyzed for the different heat flux cases. Figure 5(a) shows the transient variation in the ice volume fraction at time instants of 0, 1 and 2 minutes for input heat flux of 11 kW/m². The corresponding temperature evolution is portrayed in Fig. 5(b) for the same time instants. n-dodecane is initialized to 0 °C and heats to more than 20 °C near the surface in 2 minutes. An in-depth temperature increase is prevalent as well due to the user defined function that prescribes the in-depth heating of the fuel. The corresponding effect of heating on ice melting is also portrayed by the volume fraction of ice (Fig. 5a), where the lateral depression is shown to grow with time. It is key to note that the rate of lateral cavity generation in ice is a function of the properties of the liquid fuel and the heat input. Figure 6 shows a clear

comparison of the heating effect for the three different heat flux cases after t=2 minutes. It is observed that as the heat flux reduces, the temperature at the surface and in-depth temperature reduces. This has a direct effect on the melting profile as shown in Fig. 6(d), where at y=25 mm, the melting fronts are at locations 4.7 mm, 7 mm, and 9.8 mm from the initial x=0 mm location.

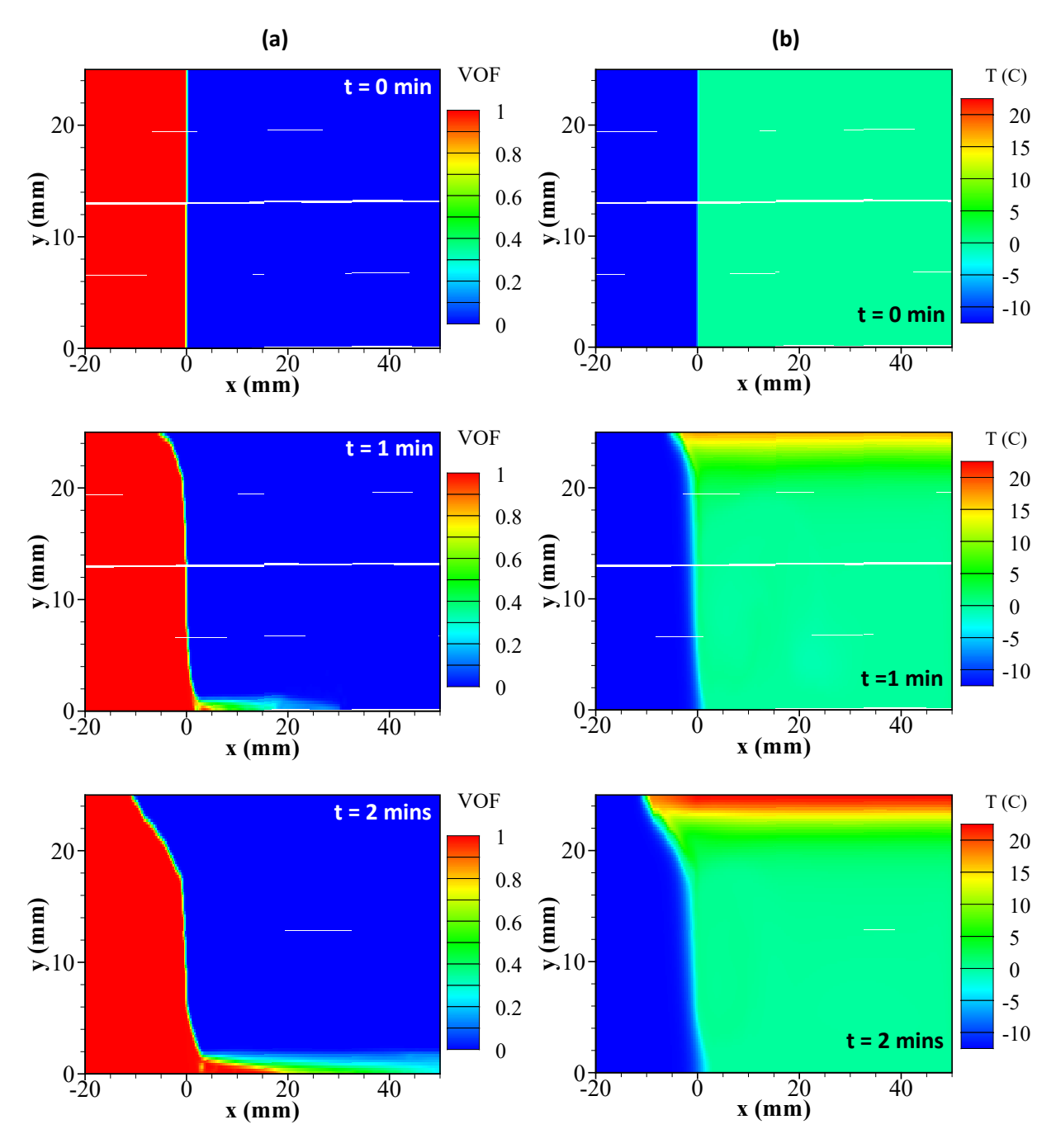


Figure 5: Profiles of (a) ice volume fraction, and (b) temperature at different time instants; heat flux = 11 kW/m^2

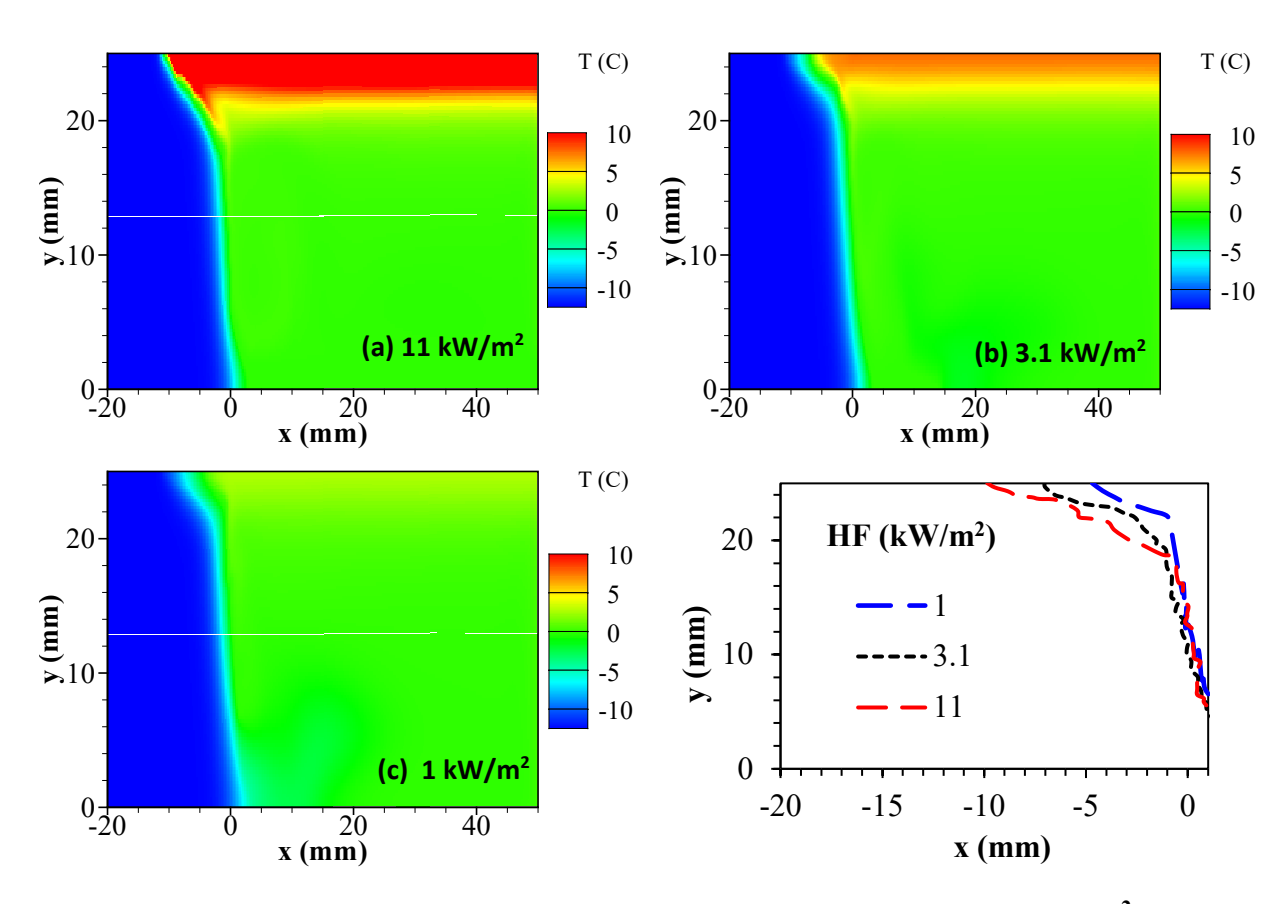


Figure 6: Temperature contour at t=2 minutes for heat flux cases (a) 11 kW/m², (b) 3.1 kW/m², (c) 1 kW/m², and (d) melting front profiles for different heat fluxes

The flow features are analyzed for the heat flux case of 11 kW/m² as shown in Fig. 7. Velocity magnitudes are higher near the water-oil interface as the melt water flows below the oil layers as shown in Fig. 7(a). This is due to the specific gravity of n-dodecane being about 0.749 the higher density melt water flows in the downward direction.

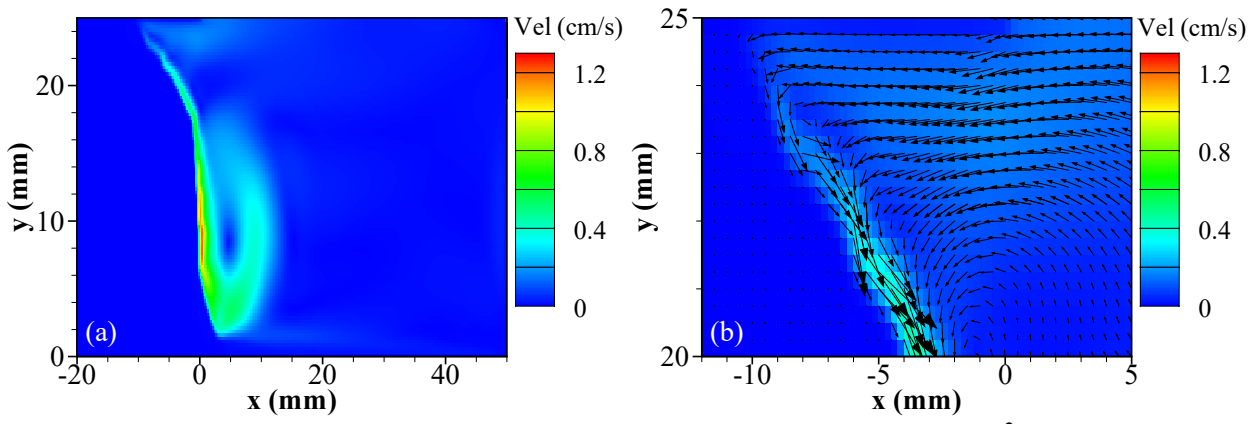


Figure 7: Velocity contour at t = 2 minutes for heat flux cases of 11 kW/m²

It is also key to note here that as n-dodecane is immiscible in water, a distinct melt layer forms at the interface between melting front and oil. Additionally, Marangoni motion is observed near the fuel surface as shown by the velocity vectors in Fig. 7(b) where surface flow towards the ice phase is seen. This is due to the temperature gradient inducing a surface tension gradient motion. This flow feature was also observed in the PIV experiments (Farahani et al. 2022) and has been predicted using the model as well.

5 Conclusion

A comprehensive two-dimensional numerical model has been developed in Ansys Fluent which simulates the in-depth heating of fuel layers due to excess heat flux using Volume of fluid method. The effect of heated fuel layers on the ice melting front is analyzed for different heat flux conditions. The model is well validated with the experimental results for different heating levels. The lateral depression in ice and the melting intrusion velocities have been predicted well using the numerical model and gives confidence in using the model for further analysis. The flow field with the melt water flowing below the less dense n-dodecane fuel layers have shown the effectiveness of the multiphase model. Additionally, the Marangoni motion near the fuel surface has also been captured by the model. The present numerical model forms a basis for developing additional studies with different fuels and varying heat conditions. This would assist in creating a map for developing a prediction correlation for oil spread in ice in the presence of surface heating. Moreover, this numerical model paves way to include multiple strategies including the effect of fuel properties, the impact of the radiation intensity, and three-dimensional models for ice melting adjacent to oil spills.

6 Acknowledgement

This material is based upon work supported by the National Science Foundation under Grant No. 1938980. Any opinions, findings and conclusions or recommendations expressed in this material are those of the authors and do not necessarily reflect those of the National Science Foundation.

7 References

- Fay, J. A., and D. P. Hoult, Physical Processes in the Spread of Oil on a Water Surface, USCG Report AD-726 281, Washington, D.C., 1971.
- Fingas, M. F., and B. P. Hollebone. "Review of behaviour of oil in freezing environments." *Marine pollution bulletin* 47.9-12 (2003): 333-340. https://doi.org/10.1016/S0025-326X(03)00210-8
- Farahani, H. F., W. U. R. Alva, A. S. Rangwala, and G. Jomaas. Convection-driven melting in an n-octane pool fire bounded by an ice wall. *Combustion and Flame* 179 (2017): 219-227. https://doi.org/10.1016/j.combustflame.2017.02.006
- Farahani, H. F., Hayashi, T., Sakaue, H., & Rangwala, A. S., Dynamics of ice melting by an immiscible liquid layer heated from above. *Experimental Thermal and Fluid Science*, (2022): 110641. https://doi.org/10.1016/j.expthermflusci.2022.110641
- Glaeser, John L., and George P. Vance. A Study of the Behavior of Oil Spills in the Arctic. *Offshore Technology Conference*. OnePetro, (1972). https://doi.org/10.4043/1551-MS

- Li, Wei, X. Liang, and J. Lin. "Mathematical Model and Computer Simulation for Oil Spill in Ice Waters Around Island Based on FLUENT." *J. Comput.* 8.4 (2013): 1027-1034. doi:10.4304/jcp.8.4.1027-1034
- Linstrom, P. J. and W. G. Mallard, Eds., *NIST Chemistry WebBook, NIST Standard Reference Database Number 69*, National Institute of Standards and Technology, Gaithersburg MD, 20899. https://doi.org/10.18434/T4D303.
- Yapa, P. D., and L. K. Dasanayaka. "State-of-the-art review of modelling oil transport and spreading in ice covered waters." (2006).
- Zhang, S., J. Zhao, J. Shi, & Y. Jiao. Surface heat budget and solar radiation allocation at a melt pond during summer in the central Arctic Ocean. *Journal of Ocean University of China*, 13(1), (2014): 45-50. https://doi.org/10.1007/s11802-014-1922-0